Copy 383

62 70369

26 p.

N63 20484

CODE-1
563330
26 p.

NASA

MEMORANDUM

LOW-SPEED INVESTIGATION OF THE EFFECTS OF HORIZONTAL-TAIL

AREA AND WING SWEEP ON THE STATIC LONGITUDINAL STABILITY

AND CONTROL CHARACTERISTICS OF AN AIRPLANE

CONFIGURATION HAVING TAIL SURFACES

OUTBOARD OF THE WING TIPS

By William C. Hayes, Jr., and William C. Sleeman, Jr.

Langley Research Center
Langley Field, Va.

CLASSIFICATION CHANGED FROM
CONFIDENTIAL TO UNCLASSIFIED--
AUTHORITY NASA-CCN 5-EFFECTIVE
17 JULY 63, JIM CARROLL
DOC. INC.

NATIONAL AERONAUTICS AND
SPACE ADMINISTRATION
WASHINGTON
June 1959

B

NATIONAL AERONAUTICS AND SPACE ADMINISTRATION

MEMORANDUM 6-11-59L

LOW-SPEED INVESTIGATION OF THE EFFECTS OF HORIZONTAL-TAIL

AREA AND WING SWEEP ON THE STATIC LONGITUDINAL STABILITY

AND CONTROL CHARACTERISTICS OF AN AIRPLANE

CONFIGURATION HAVING TAIL SURFACES

OUTBOARD OF THE WING TIPS*

By William C. Hayes, Jr., and William C. Sleeman, Jr.

SUMMARY

A low-speed investigation was conducted in the Langley 300-MPH 7- by 10-foot tunnel to determine the static longitudinal stability and control characteristics of a model having tail surfaces located outboard and rearward of the wing tips. The wing of the model had an aspect ratio of 1.00 and could be adjusted to give leading-edge sweep angles of 60°, 65°, and 70°. Four horizontal tails of different size, in which the area varied from 10 to 27.8 percent of the wing area, were used in the tests. Very brief tests were conducted to assess the directional stability characteristics of the model for angles of attack up to 30°.

The test results indicated that the outboard horizontal tail was an effective pitch control over the test angle-of-attack range; however, for the basic model with the 70° swept wing, there was an appreciable loss in longitudinal stability for lift coefficients above approximately 0.70. A reduction in wing sweep angle to 60° improved the longitudinal stability at high lift coefficients and reduced the variation of stability with lift coefficient throughout the test angle-of-attack range.

Directional stability of the model was high throughout the test angle-of-attack range, with the stability at an angle of attack of 30° greater than at low angles of attack.

*Title, Unclassified.

CONFIDENTIAL

INTRODUCTION

Airplane design trends which result primarily from the quest for high lift-drag ratios at supersonic speeds have given rise to troublesome stability problems at moderate and high angles of attack. A possible airplane configuration which may alleviate the stability problems encountered on many high-speed configurations yet may maintain attractive performance at supersonic speeds has been suggested. The basic concepts and some supporting experimental results are presented in reference 1 for an airplane arrangement having the horizontal- and vertical-tail surfaces mounted on slender bodies and located outboard and rearward of the wing tips.

Tests of an outboard-tail configuration at Mach numbers from 2.30 to 3.51 reported in reference 2 indicated that relatively high values of lift-drag ratio for trimmed conditions could be obtained on an arrangement which also had good directional stability characteristics through the angle-of-attack range. The results of reference 2 and subsonic data of reference 1, however, indicated possible problems of longitudinal stability at moderate and high angles of attack. The present low-speed investigation was therefore undertaken to study the longitudinal stability characteristics of a simplified model, geometrically similar in most respects to the model of reference 2, and to explore means for improving its longitudinal stability at high angles of attack.

Longitudinal stability characteristics of the basic and modified model were obtained over an angle-of-attack range up to approximately 30°. Effects on stability of both wing sweep and horizontal-tail area were studied for wing leading-edge sweep angles of 60°, 65°, and 70° and for horizontal-tail areas that were 10, 15, 20, and 27.8 percent of the wing area.

SYMBOLS

The system of axes used in this investigation is shown in figure 1 together with an indication of the positive direction of forces, moments, and angular displacements. The moment reference center was located 52.45 inches from the nose and corresponded to the 50-percent mean aerodynamic chord of the 70° swept wing. All coefficients presented herein are based on the area, span, and mean aerodynamic chord of the composite plan form of the 70° swept wing and largest horizontal tail. The symbols used are defined as follows:

CONFIDENTIAL

C_L lift coefficient, $\dfrac{\text{Lift}}{qS}$

C_D drag coefficient, $\dfrac{\text{Drag}}{qS}$

C_Y lateral-force coefficient, $\dfrac{\text{Lateral force}}{qS}$

C_l rolling-moment coefficient, $\dfrac{\text{Rolling moment}}{qSb}$

C_m pitching-moment coefficient, $\dfrac{\text{Pitching moment}}{qS\bar{c}}$

C_n yawing-moment coefficient, $\dfrac{\text{Yawing moment}}{qSb}$

b reference span of wing plus span of largest horizontal tail, 4.00 ft

$\bar{c}$ reference mean aerodynamic chord based on combination of wing and largest horizontal tail, 2.16 ft

$\bar{c}_h$ mean aerodynamic chord of horizontal tail

$\bar{c}_w$ mean aerodynamic chord of wing alone

q free-stream dynamic pressure, lb/sq ft

S reference area of basic wing plus area of largest horizontal tail, 6.96 sq ft

S_h plan-form area of horizontal tail

S_w plan-form area of wing alone

α angle of attack of fuselage center line, deg

β angle of sideslip, deg

Λ angle of sweepback of wing leading edge, deg

δ_h deflection of horizontal tail with respect to fuselage center line, deg

$$C_{Y_\beta} = \frac{\partial C_Y}{\partial \beta}$$

$$C_{l_\beta} = \frac{\partial C_l}{\partial \beta}$$

$$C_{n_\beta} = \frac{\partial C_n}{\partial \beta}$$

MODEL AND APPARATUS

The model (figs. 2 to 5) used in this investigation consisted of mahogany central and outboard bodies and aluminum wing and tail surfaces. The basic wing was swept 70° at the leading edge and had an aspect ratio of 1.00, a taper ratio of 0.39, and a flat-plate airfoil section $0.017\bar{c}$ thick with a faired leading edge and beveled trailing edge. The basic horizontal tail was swept 60° at the leading edge and had an area 27.8 percent of the basic wing area S_w. The wing leading-edge sweep could be varied, whereas the wing span and area remained constant. Geometric characteristics of each wing plan form used are presented in table I. In addition to the variation of leading-edge sweep angle a leading-edge extension of 4 inches in the free-stream direction could be attached to the basic wing. All horizontal tails had the same plan form, but area ratios $S_h/S_w = 0.278$, 0.20, 0.15, and 0.10. The same horizontal tails were used with all wings; however, for a few tests, the horizontal tails were moved forward 4 inches when the configuration with the 4-inch leading-edge extension was tested. All horizontal tails could be deflected about a hinge axis through the 25-percent mean aerodynamic chord of the horizontal tail and perpendicular to the center line of the outboard body. Vertical tails which were identical to the basic horizontal tail were used in all tests.

TESTS AND CORRECTIONS

The present investigation was conducted in the Langley 300-MPH 7- by 10-foot tunnel at a dynamic pressure of 57.5 pounds per square foot which corresponded to an airspeed of about 150 miles per hour. The test conditions produced a test Reynolds number of approximately 3.0×10^6 based on the mean aerodynamic chord of the combined basic wing plus basic horizontal tail. The angle-of-attack range was from -4° to approximately 30°. Two tests were made through the angle-of-attack range with the angle of sideslip at 5° and -5°.

Blockage corrections as computed by the method of reference 3 were applied to the free-stream dynamic pressure. Jet-boundary corrections as computed by the method of reference 4, with the combined basic wing and horizontal tail considered as a single lifting surface, were added to the angles of attack and drag coefficients. Corrections for tunnel buoyancy effects were also applied. No corrections have been applied to account for the base drag of the model fuselage.

DISCUSSION

Inasmuch as the tail surfaces were assumed to contribute a positive increment of lift to the total airplane lift in trimmed supersonic flight, the aerodynamic coefficients for all configurations are based on the composite wing area of the basic configuration; that is, the area of the 70° swept wing plus the area of the largest horizontal tail $\left(S_h/S_w = 0.278\right)$. This configuration is similar in plan form to the supersonic model of reference 2. The moment reference location was at the 50-percent mean aerodynamic chord of the wing of the basic configuration $\left(\Lambda = 70^\circ\right)$, that is, 52.45 inches from the fuselage nose, and was assumed to be a reasonable airplane center-of-gravity location. Since the position of the outboard bodies remained fixed with respect to the fuselage for all configurations, it was believed that this moment reference location would be satisfactory for all tests.

Effect of Horizontal-Tail Deflection

The effects of horizontal-tail deflection on the aerodynamic characteristics of the model are presented in figure 6. These results show a progressive decrease in lift coefficient as the horizontal-tail deflection is varied from 0° to -12° at a given angle of attack; however, the increases in drag coefficient associated with the larger negative deflection at a given lift coefficient are not so pronounced. This characteristic is consistent with the results of references 1 and 2 and occurs as a result of the field of upflow in the vicinity of the horizontal tail.

The pitching-moment characteristics presented in figure 6 show that the horizontal tail provides an appreciable stability contribution at low and moderate angles of attack. In addition the tail is an effective longitudinal control to at least 30° angle of attack as is indicated by the fact that the stabilizer effectiveness $\partial C_m/\partial \delta_h$ generally is about the same at the highest angles of attack as at 0°. The pitching-moment curve for the stabilizer setting of 0° indicates a loss in stability at the highest angles of attack, which is not noted at the other stabilizer angles. Apparently this loss in stability results from tail stall since

the expected relief of the condition at negative tail deflections is
verified by the remaining pitching-moment curves.

A significant reduction in longitudinal stability occurs for all
stabilizer settings at angles of attack above about 16° $(C_L = 0.70)$ and
is believed to be a result of changes in the flow angularity at the tail
as high angles of attack are approached. A loss in effective upwash at
the tails would be expected as the wing-tip vortex moves up and inboard
relative to the wing chord plane as the angle of attack is increased.
The problem of possible stability losses due to decreases in upwash at
high angles of attack for this configuration prompted the present inves-
tigation of effects of horizontal-tail area and wing sweep angle.

L
3
8
2

Effect of Horizontal-Tail Area

The effects of variation of the horizontal-tail area for the 70° swept-
wing model are shown in figure 7. Decreases in the horizontal-tail area
were accompanied by reduced lift coefficients at given angles of attack
and increased drag coefficients at a given lift coefficient; however,
these coefficients were calculated from the reference area of the basic
configuration; whereas the actual area decreased with decreasing tail
area.

The expected reduction in longitudinal stability at low lift with
decreasing tail area is shown in the results of figures 7 to 9. Of more
importance, however, is the change in stability which occurred throughout
the angle-of-attack range for each tail. A reduction in tail area had
little effect on the variation of stability with lift coefficient, and
with the smallest tail (fig. 7) there was still a significant reduction
in stability at angles of attack above about 15°. A reduction in tail
area might be expected to eliminate the change in stability with lift
coefficient by virtue of the fact that the tail-off pitching moments do
not indicate significant stability loss at high angles of attack (fig. 6).
This improvement in stability variation with lift was not realized for
the smaller tails, possibly because of the nature of the upwash variation
across the tail span. The maximum local upwash might be expected near
the tail root and the average upwash across the whole tail span, of course,
would increase as the tail span (or area) is reduced. Thus, the change
in upwash (resulting from displacement of the wing-tip vortex) as the
angle of attack is increased is greater for the smaller tails and occurs
at a lower angle of attack than for the larger tails. Therefore, the
greater upwash changes apparently compensate for the smaller tail area
so that improvements in the pitching-moment variation with lift were not
realized with the smaller tails.

Effect of Wing Leading-Edge Sweep

The results of figure 10(a) show fairly small effects of wing sweep for the configuration without the horizontal tail. Pitching-moment characteristics with the horizontal tail on show virtually no reduction in stability at low and moderate lift coefficients with decreasing wing sweep for a given tail size. At the higher angles of attack, decreasing wing sweep was accompanied by increased stability (fig. 10(b)). The pitching-moment results obtained with a stabilizer setting of -9° show that reduction of wing sweep also effected slightly smaller stability changes with angle of attack. (This stabilizer setting is chosen for discussion, inasmuch as the stability loss shown for the 0° setting at high angles of attack was probably due to tail stall as mentioned previously.) Results with the 60° swept wing and horizontal tail $\left(S_h/S_w = 0.15, \quad \delta_h = -9^\circ\right)$ show very little change in stability with lift coefficient through the entire angle-of-attack range (fig. 9).

Effect of Extended Wing Leading Edge

Characteristics of the model with the 70° swept leading edge with a constant 4-inch extension to the wing chord are presented in figure 11 for two tail areas $\left(S_h/S_w = 0.278 \text{ and } 0.150\right)$ and in figure 12 for the large horizontal tail $\left(S_h/S_w = 0.278\right)$ moved 4 inches forward on the outboard body. No improvements in pitching-moment characteristics such as were obtained by using a lower wing sweep and smaller tail (fig. 9) were indicated. The results of figure 12 do show, however, that the characteristics of the basic model could be improved slightly by decreasing the wing aspect ratio and moving the horizontal tail forward.

Lateral Stability Derivatives

Although the present study was concerned almost exclusively with problems of longitudinal stability and control, a very brief evaluation of lateral stability was made for the basic configurations $\left(\Lambda = 70^\circ,\right.$ $\left. S_h/S_w = 0.278, \quad \delta_h = -9^\circ\right)$. These results are presented in figure 13 and show the model to be directionally stable throughout the angle-of-attack range (to 30°) with the stability increasing markedly above an angle of attack of about 10°. This trend has been noted in other outboard-tail models and is probably due primarily to the increased stability of the tail-off configuration (ref. 1).

The variation of C_{l_β} with angle of attack indicates negative effective dihedral at the lower angles of attack as a result of the contribution

CONFIDENTIAL

of the horizontal tails at negative deflections and their long moment arms. A theoretical estimation of C_{l_β} at an angle of attack of 0° indicated positive increments of C_{l_β} contributed by the horizontal tail because of the tail sweep and aspect ratio when at a negative angle of attack (ref. 5) and because of the interference effect of the vertical tail (ref. 6). Inasmuch as the wings were at an angle of attack of 0°, the only negative contribution to C_{l_β} was from the vertical tails. The calculated value of C_{l_β} from the aforementioned considerations was 0.00091 as compared with an experimental value of 0.00146 (fig. 13). Although reference 6 pertains strictly to the conventional center tail assemblies, it was believed that the interference effect of the vertical tail on the horizontal tail would produce a small amount of positive rolling moment due to sideslip, which in turn, would be magnified by the long moment arm of the present model. At angles of attack above approximately 12.5° (the trim angle of attack for this configuration), C_{l_β} is negative.

CONCLUSIONS

A low-speed investigation of effects of horizontal-tail size and wing sweep on the longitudinal characteristics of an airplane configuration having tail surfaces outboard of the wing tips indicated the following results:

1. The outboard horizontal tail was an effective pitch control over the test angle-of-attack range and would be expected to provide longitudinal trim for angles of attack up to 30°.

2. Pitching-moment data for the 70° swept-wing model with a tail area of 0.278 of the wing area indicated an appreciable loss in longitudinal stability at a lift coefficient above approximately 0.70. Reductions in horizontal-tail area from that of the basic model were not particularly effective in reducing the variation of longitudinal stability with lift coefficient.

3. A progressive reduction in wing leading-edge sweep angle from 70° to 60° had little effect on the pitching-moment characteristics of the configuration without the horizontal tail; however, with the horizontal tail on, reductions in sweep angle increased the stability at high lift coefficients and decreased the variation of longitudinal stability with angle of attack. A configuration having very little change of stability with angle of attack was achieved by use of the 60° swept wing and small tails having an area 15 percent of the wing area and a tail deflection of -9°.

CONFIDENTIAL

!B

4. Directional stability of the model was high throughout the test angle-of-attack range, with the stability at an angle of attack of 30° greater than at low angles of attack.

Langley Research Center,
National Aeronautics and Space Administration,
Langley Field, Va., March 16, 1959.

REFERENCES

1. Sleeman, William C., Jr.: Preliminary Study of Airplane Configurations Having Tail Surfaces Outboard of the Wing Tips. NACA RM L58B06, 1958.

2. Church, James D., Hayes, William C., Jr., and Sleeman, William C., Jr.: Investigation of the Aerodynamic Characteristics of an Airplane Configuration Having Tail Surfaces Outboard of the Wing Tips at Mach Numbers of 2.30, 2.97, and 3.51. NACA RM L58C25, 1958.

3. Herriot, John G.: Blockage Corrections for Three-Dimensional-Flow Closed-Throat Wind Tunnels, With Consideration of the Effect of Compressibility. NACA Rep. 995, 1950. (Supersedes NACA RM A7B28.)

4. Gillis, Clarence L., Polhamus, Edward C., and Gray, Joseph L., Jr.: Charts for Determining Jet-Boundary Corrections for Complete Models in 7- by 10-Foot Closed Rectangular Wind Tunnels. WR-L-123, 1945. (Formerly NACA ARR L5G31.)

5. Polhamus, Edward C., and Sleeman, William C., Jr.: The Rolling Moment Due to Sideslip of Swept Wings at Subsonic and Transonic Speeds. NACA RM L54L01, 1955.

6. Queijo, M. J., and Riley, Donald R.: Calculated Subsonic Span Loads and Resulting Stability Derivatives of Unswept and 45° Sweptback Tail Surfaces in Sideslip and in Steady Roll. NACA TN 3245, 1954.

CONFIDENTIAL

TABLE I

GEOMETRIC CHARACTERISTICS OF WINGS ALONE

Λ, deg	$\bar{c}_W$, in.	Root chord, in.	S_W, sq in.	Taper ratio	Aspect ratio
60	28.31	33.13	784.00	0.691	1.000
65	28.76	36.01	784.00	.555	1.000
70	29.79	40.23	784.00	.392	1.000
70	33.53	44.23	895.45	.446	.875

All wings had 1/2-inch-thick flat-plate airfoil sections with faired leading edge and beveled trailing edge.
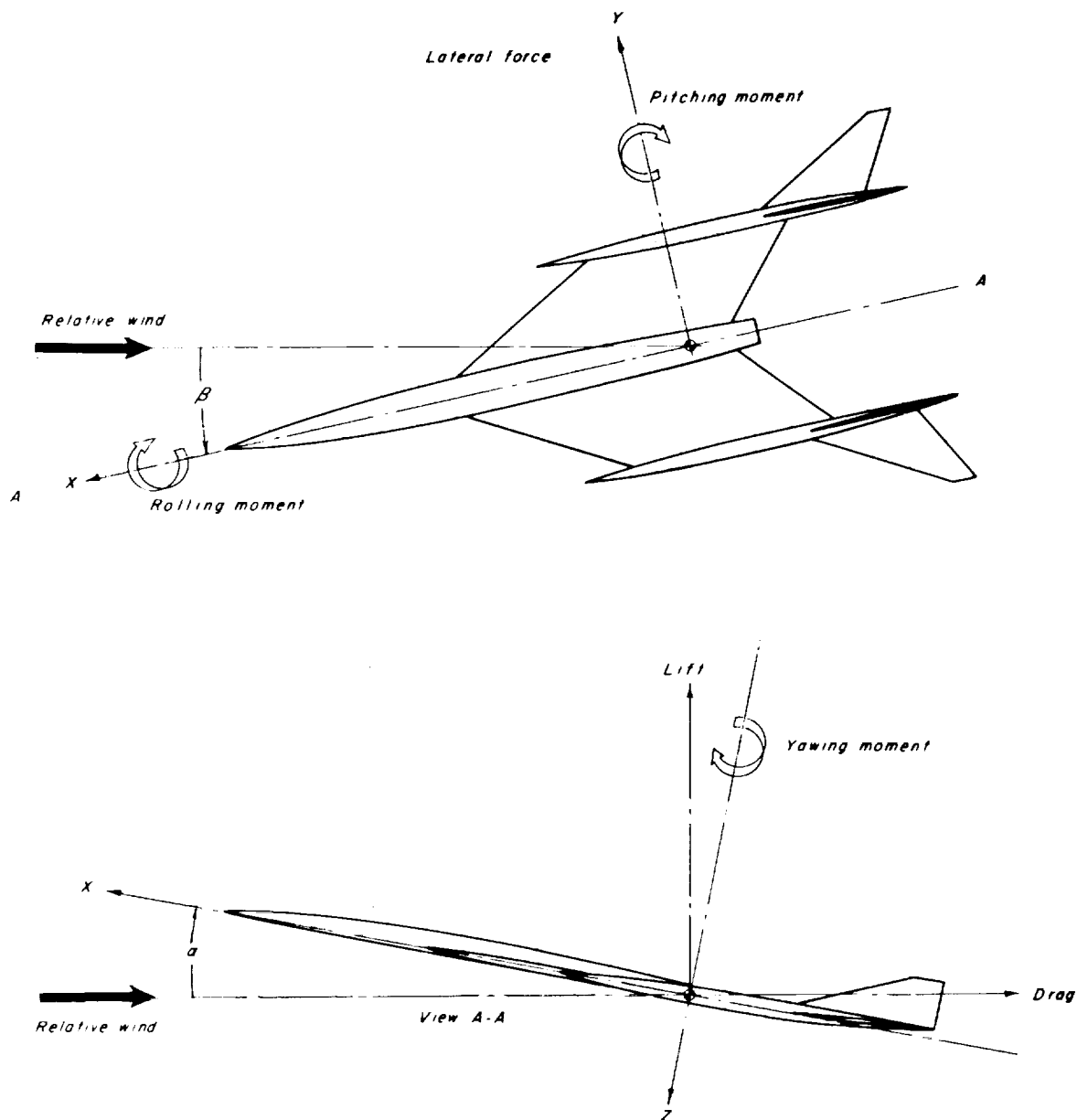
Figure 1.- System of axes. Arrows indicate positive direction of forces,
moments, and angles.
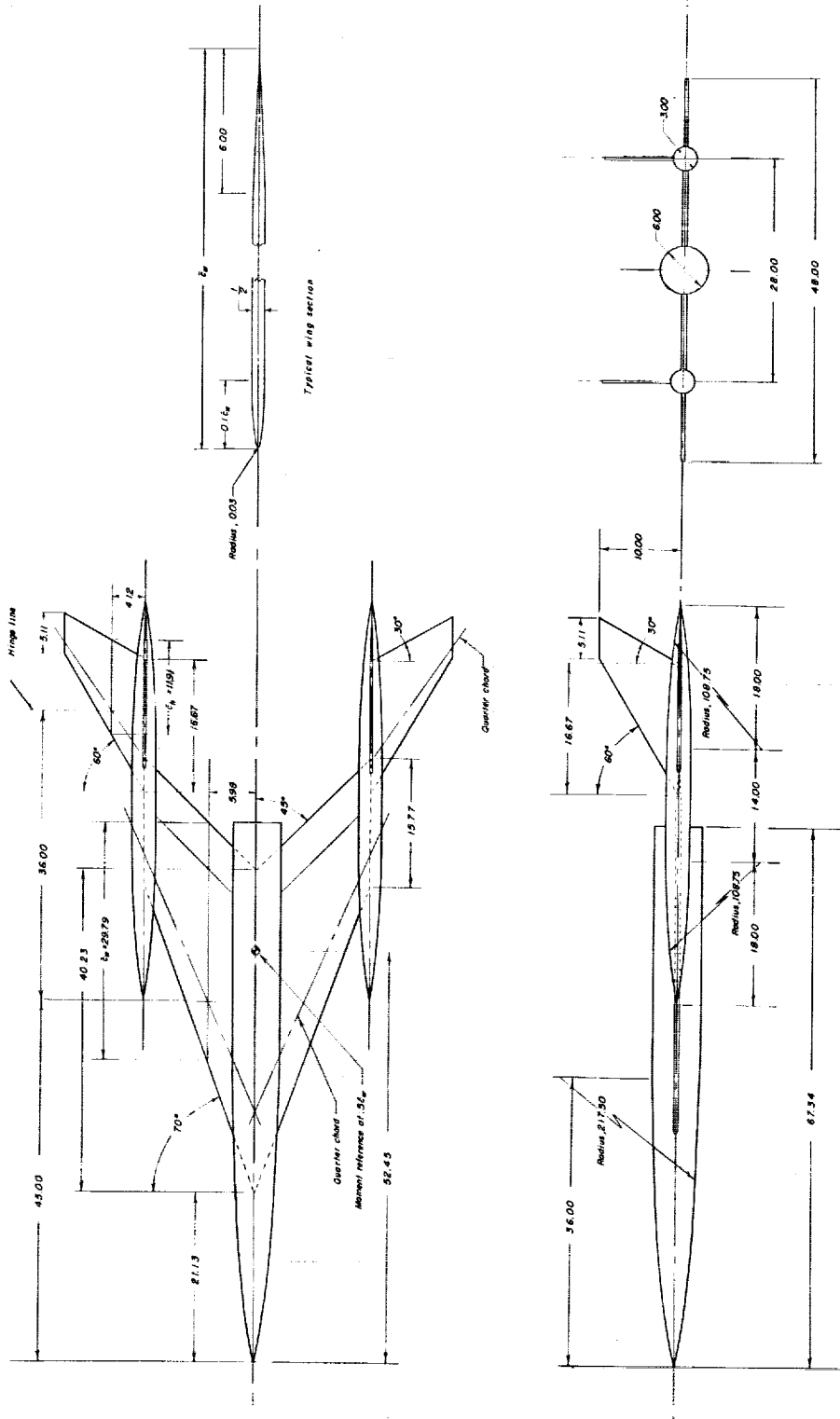
Figure 2.- Sketch of 70° swept-wing model with tail area 0.278 wing area. All dimensions in inches.
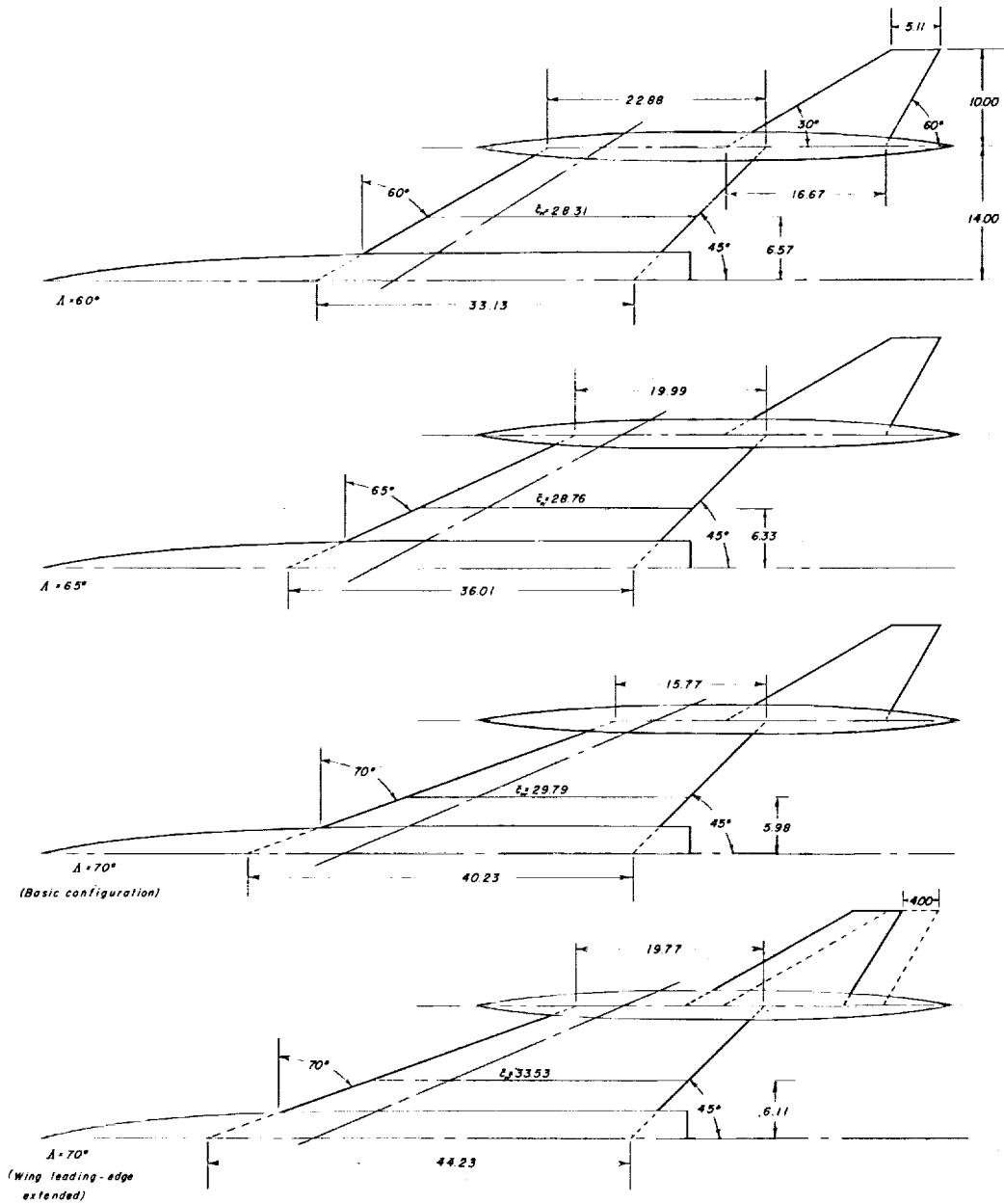
Figure 3.- Sketches of wings tested. All dimensions in inches.
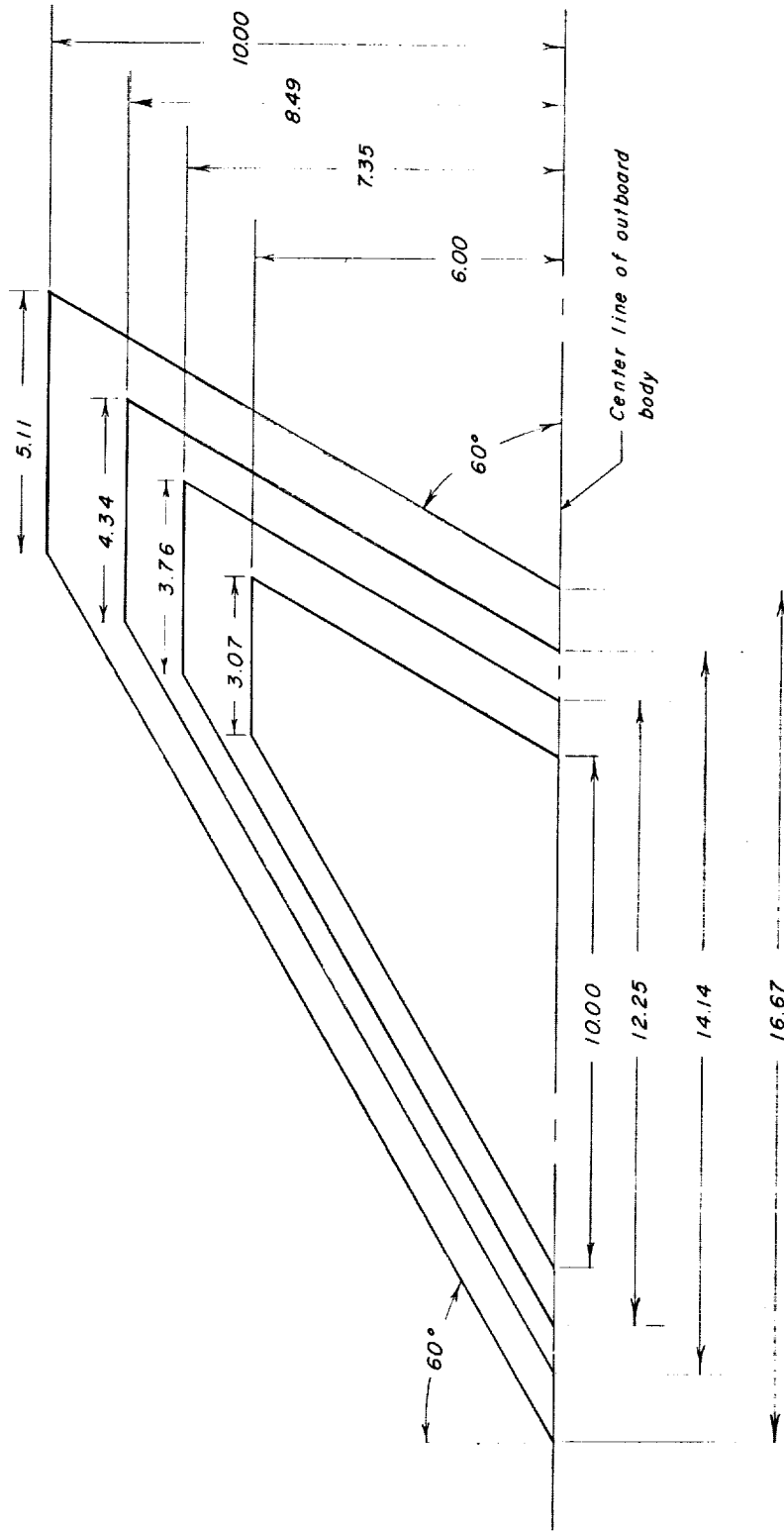
Figure 4.- Plan views of semispan horizontal tails used. All dimensions in inches.

L-382
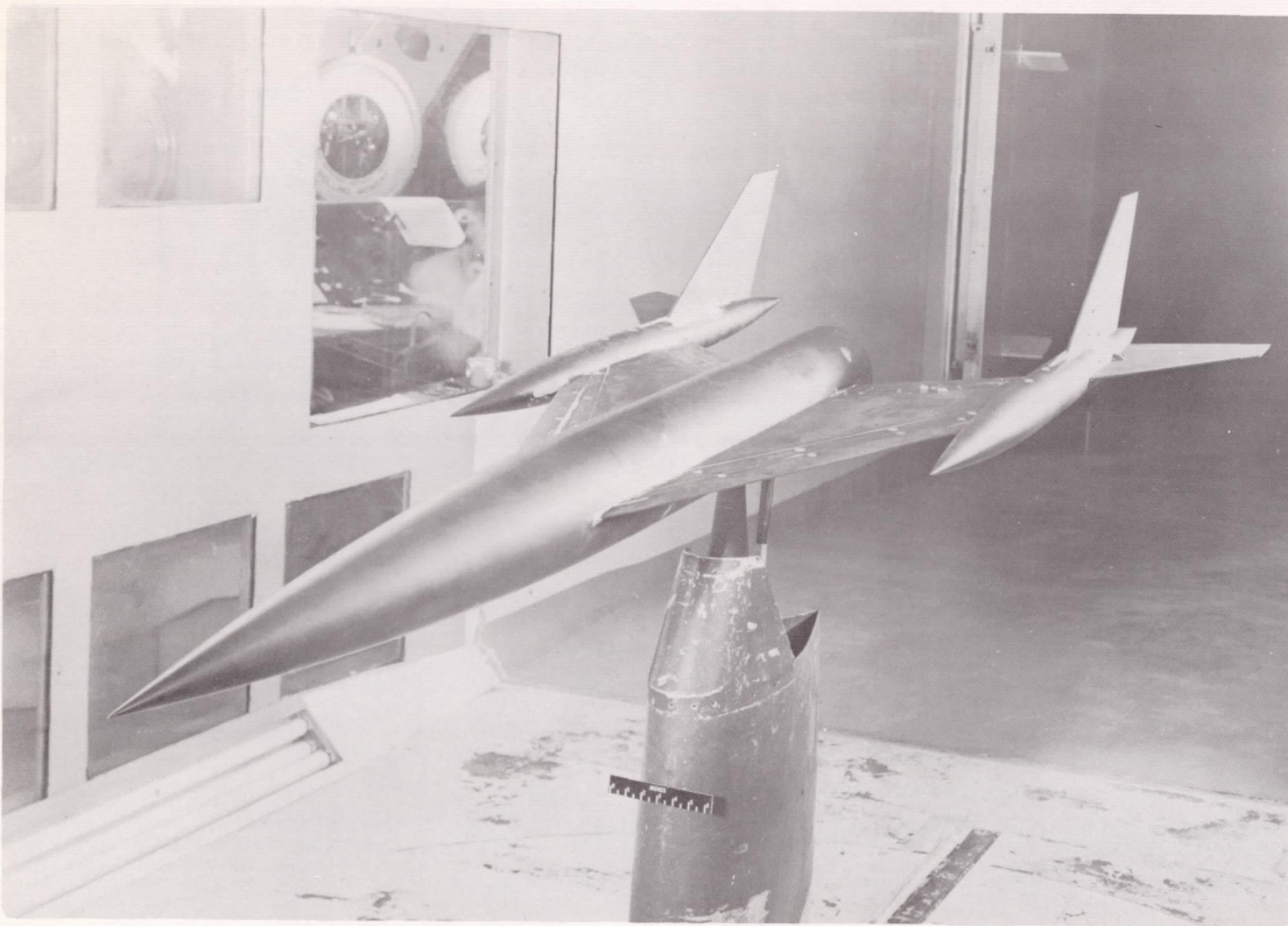
L-57-4567

Figure 5.- Photograph of the model installed in the Langley 300-MPH 7- by 10-foot tunnel.

15

CONFIDENTIAL

L-382
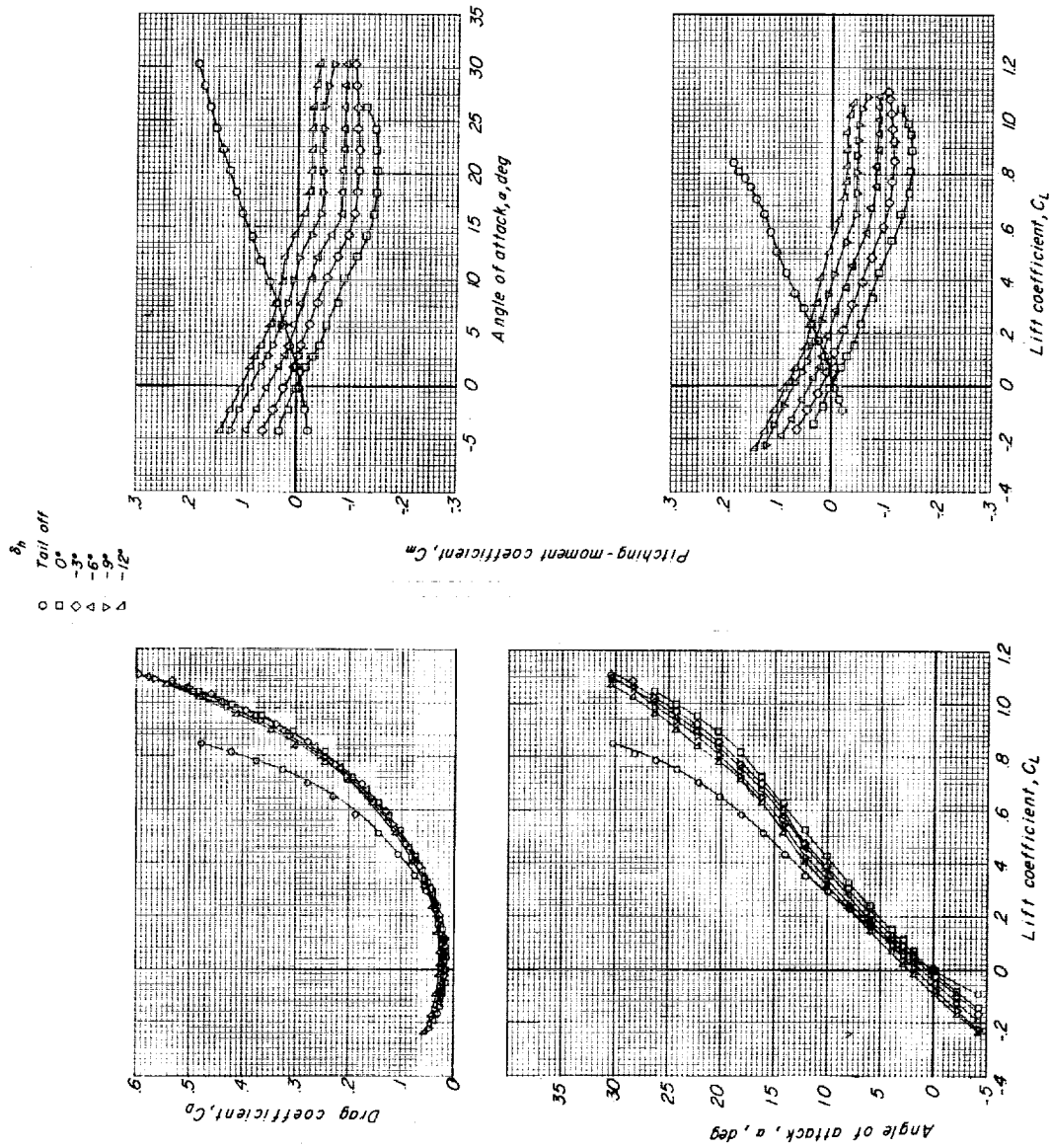
Figure 6.- Effect of horizontal-tail deflection on longitudinal aerodynamic characteristics. $\Lambda = 70^{\circ}$; $S_h/S_w = 0.278$.
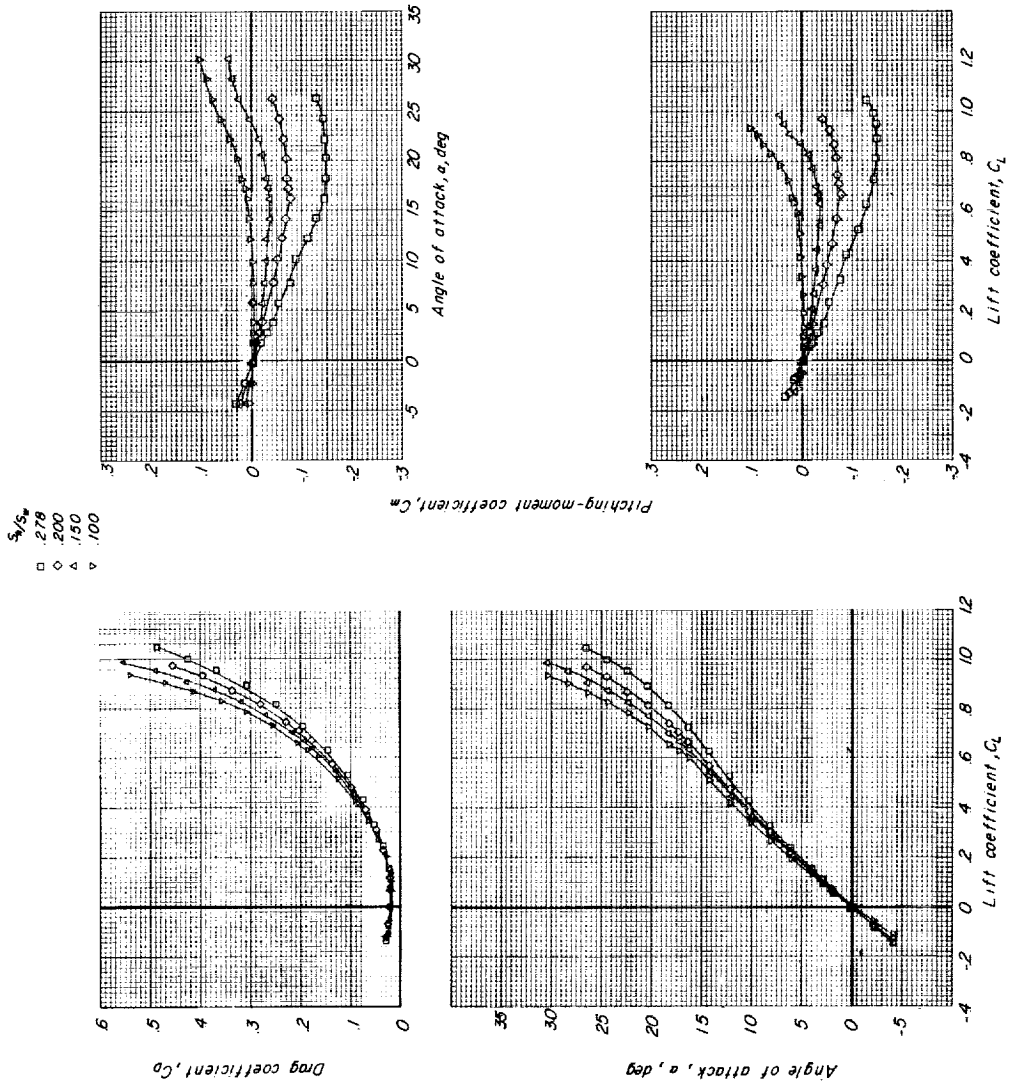
Figure 7.- Effect of horizontal-tail area on longitudinal aerodynamic characteristics. $\Lambda = 70°$.

(a) $\delta_h = 0°$.
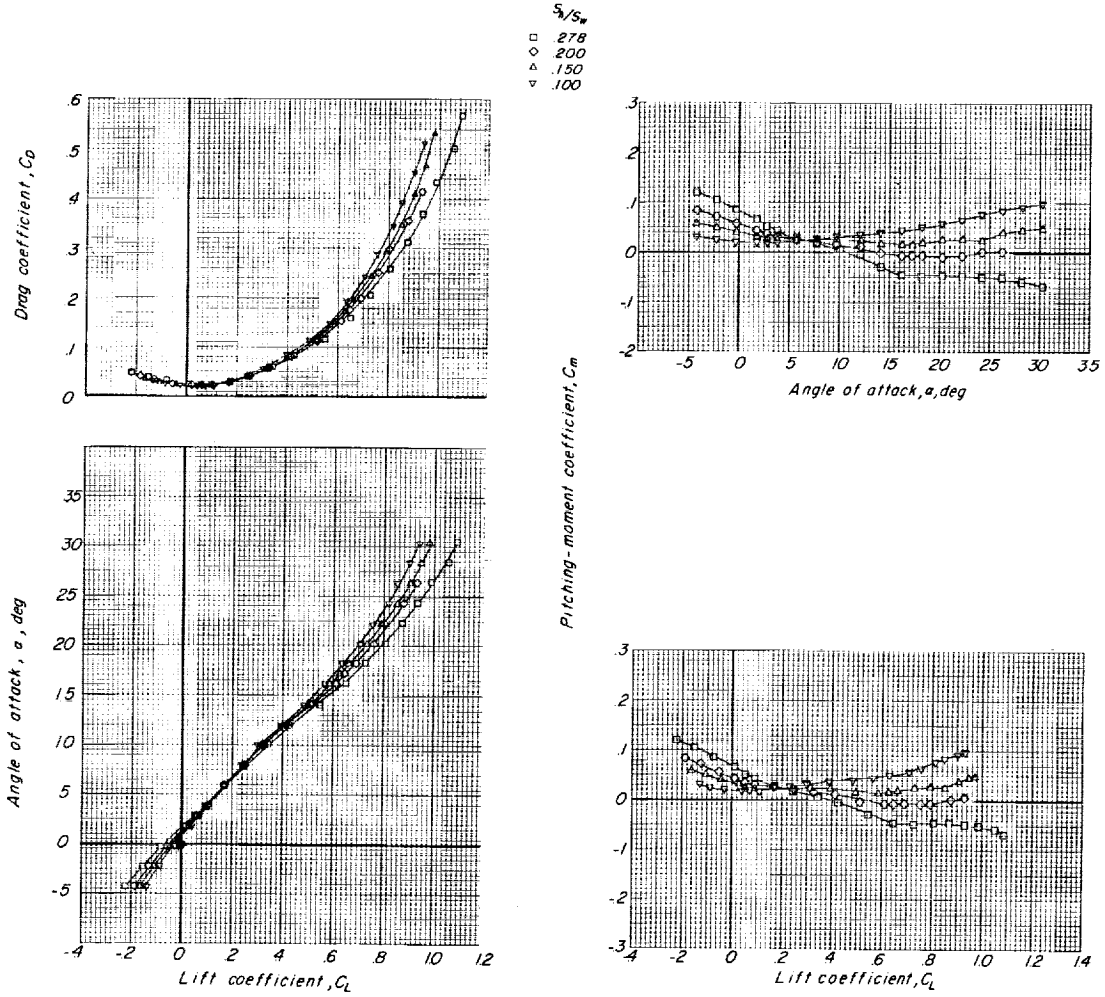
(b) δ_h = -9°.

Figure 7.- Concluded.
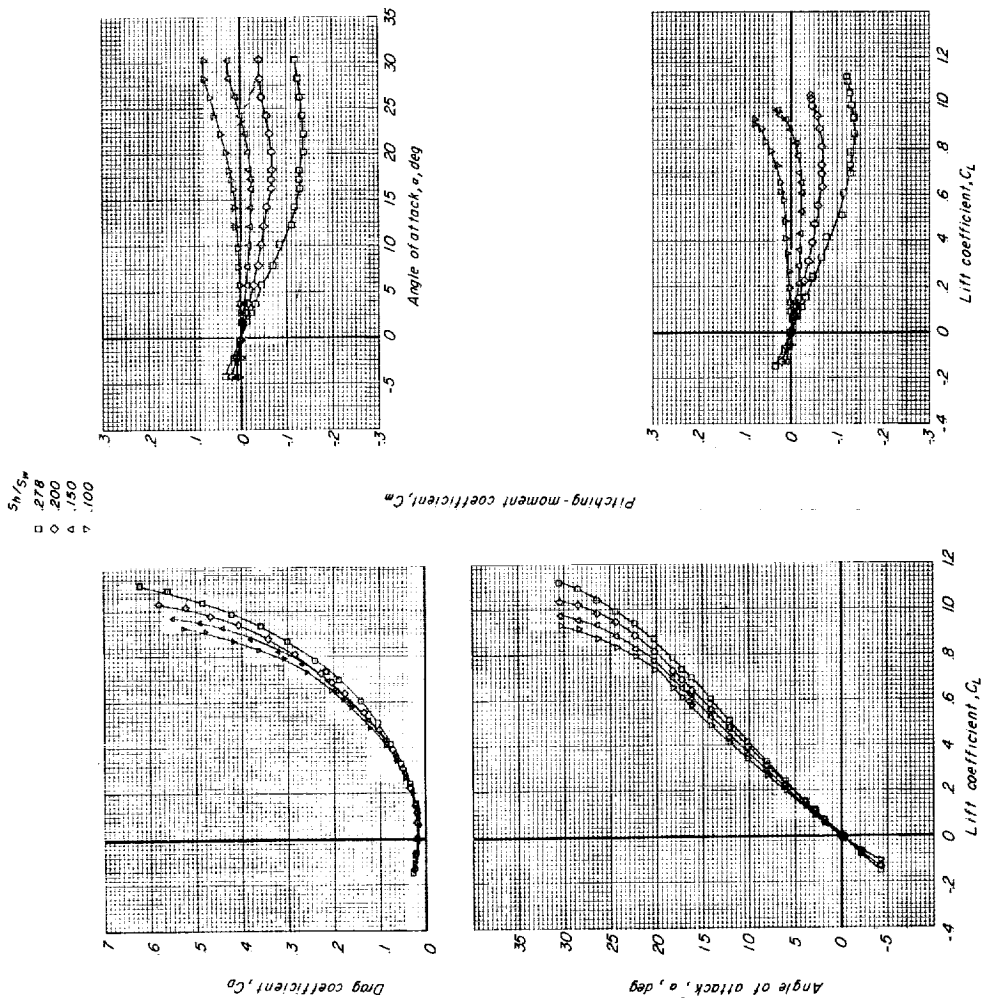
(a) $\delta_h = 0°$.

Figure 8.- Effect of horizontal-tail area on longitudinal aerodynamic characteristics. $\Lambda = 65°$.
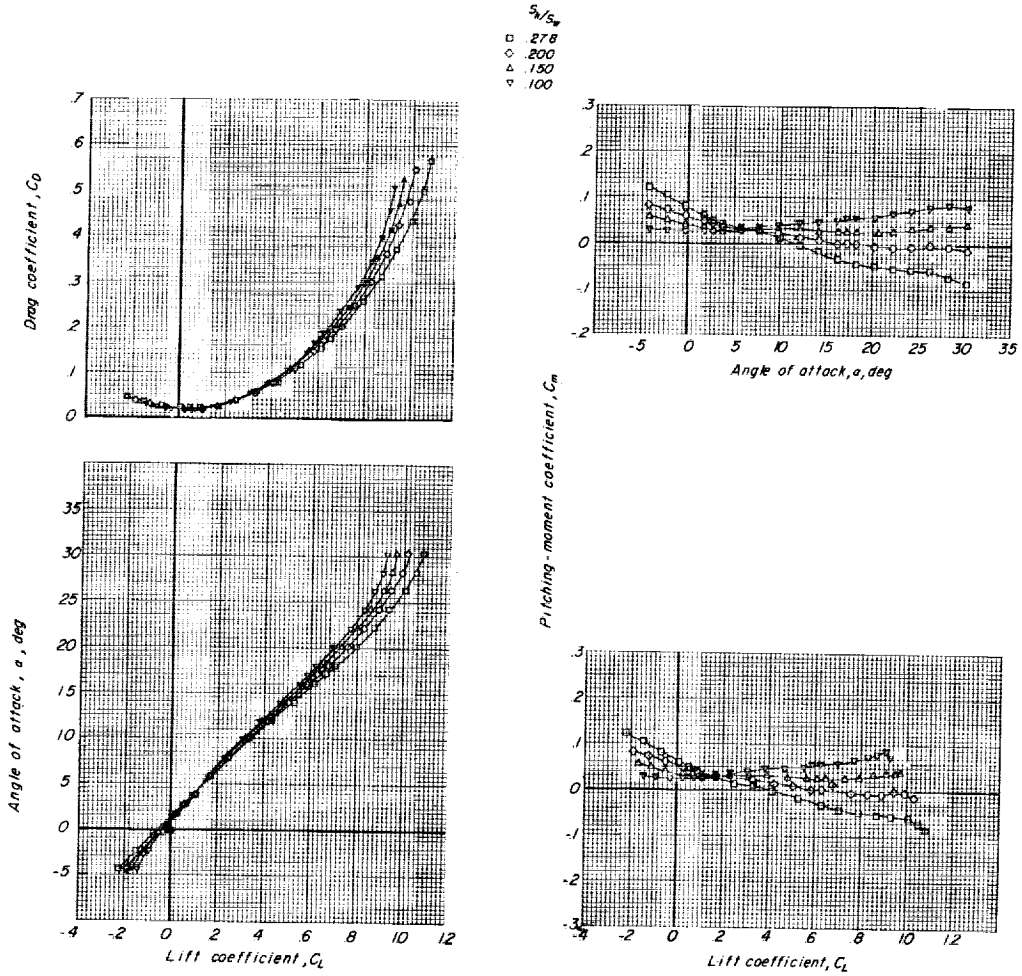
(b) $\delta_h = -9°$.

Figure 8.- Concluded.
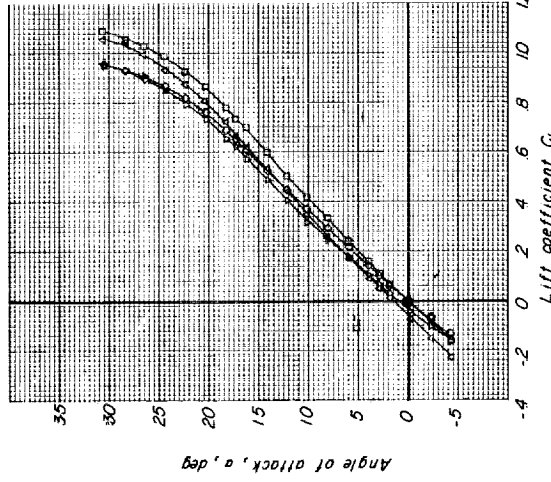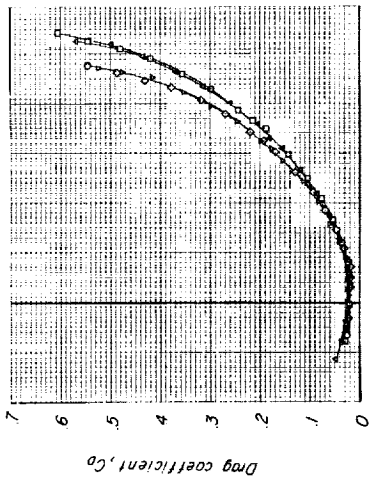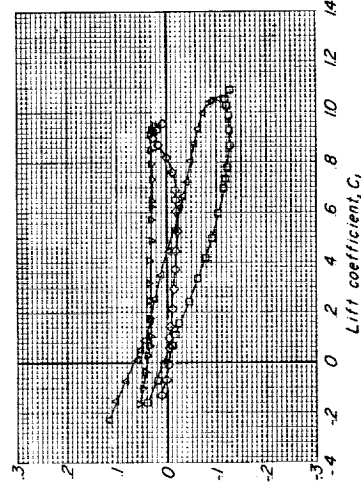
L-382

Figure 9.- Effect of horizontal-tail area and deflection on longitudinal aerodynamic charac-
teristics. $\Lambda = 60°$.
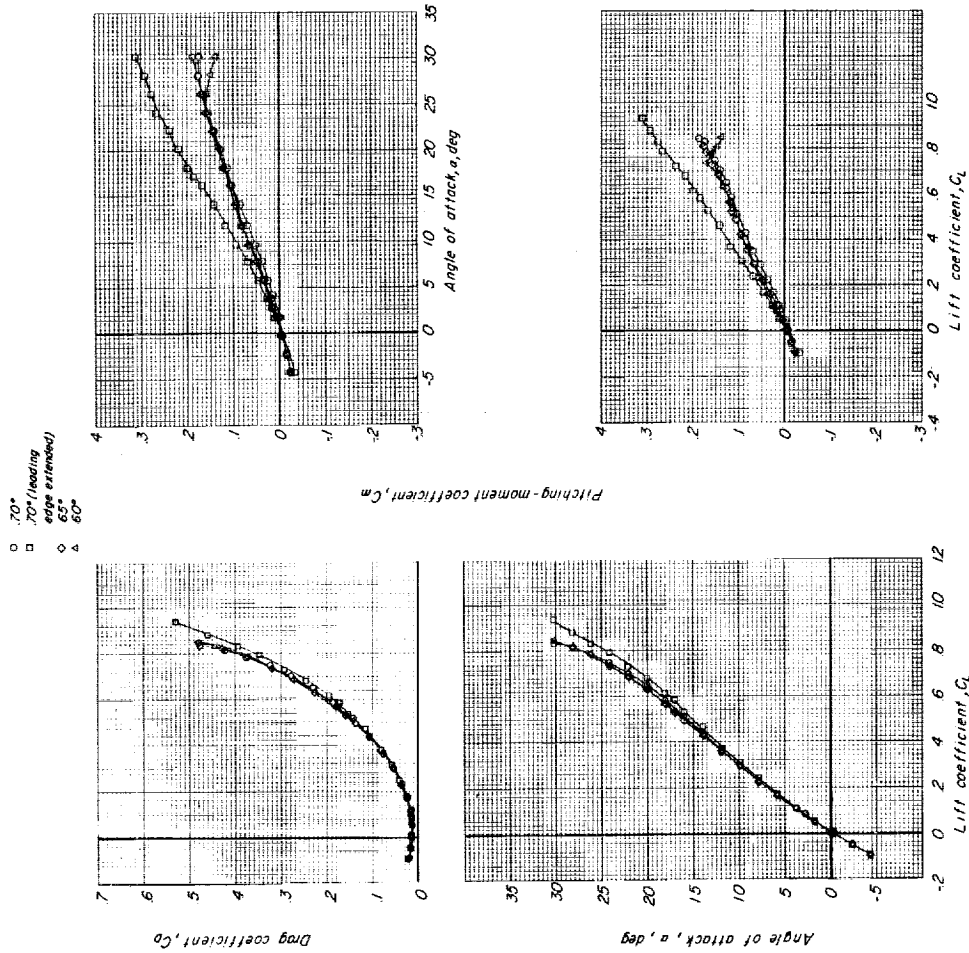
L-382

(a) Horizontal tail off.

Figure 10.- Effect of wing leading-edge sweep on longitudinal aerodynamic characteristics.

Λ, deg
□   70
◇   65
△   60

Angle of attack, a, deg

C_L
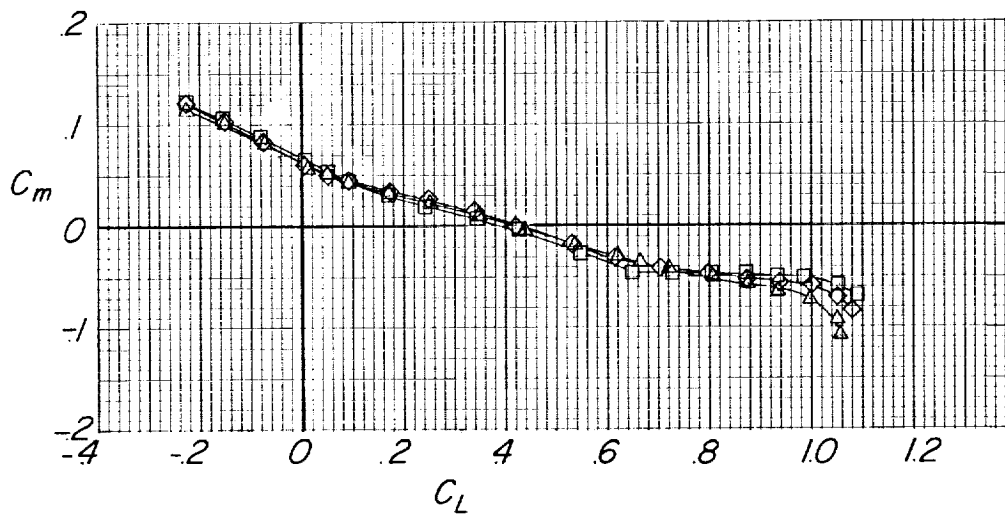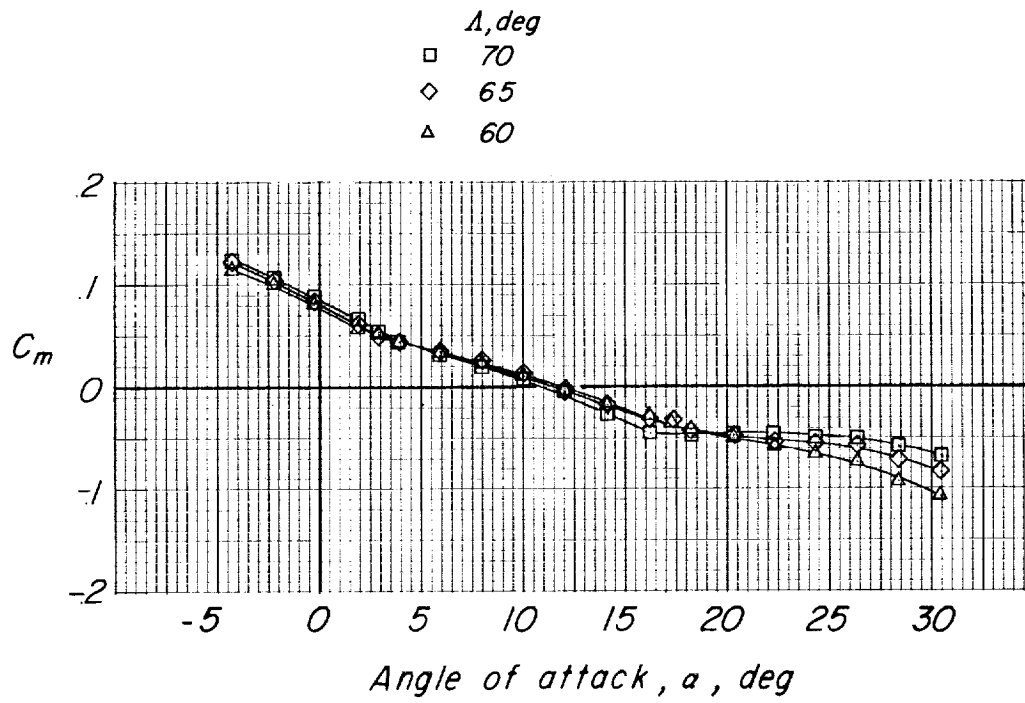
(b) $\delta_h = -9°$; $S_h/S_w = 0.278$.

Figure 10.- Concluded.

CONFIDENTIAL

L-382
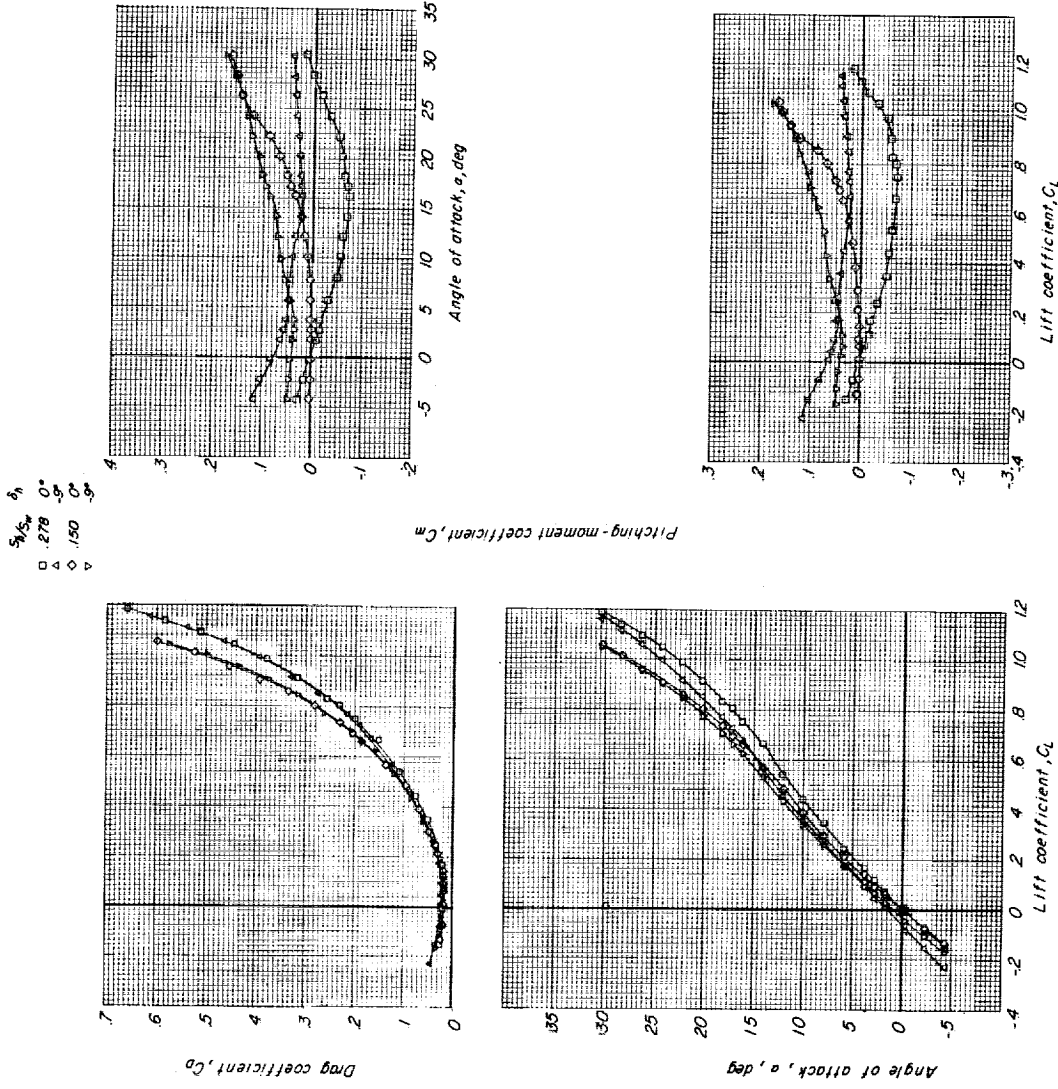
Figure 11.- Effect of horizontal-tail area and deflection on longitudinal aerodynamic charac-
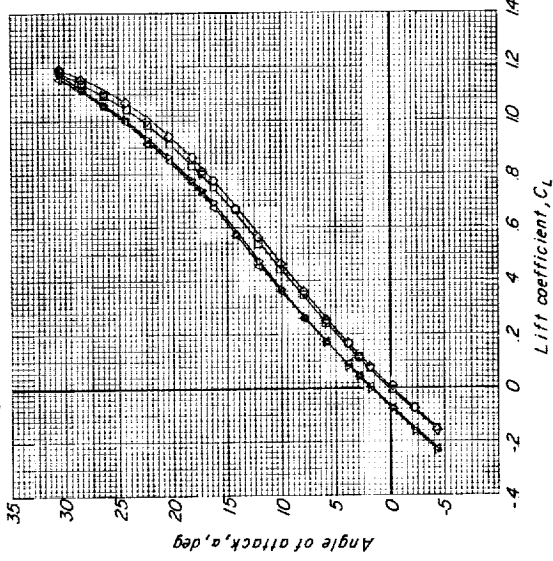teristics. $\Lambda = 70°$ (leading edge extended).
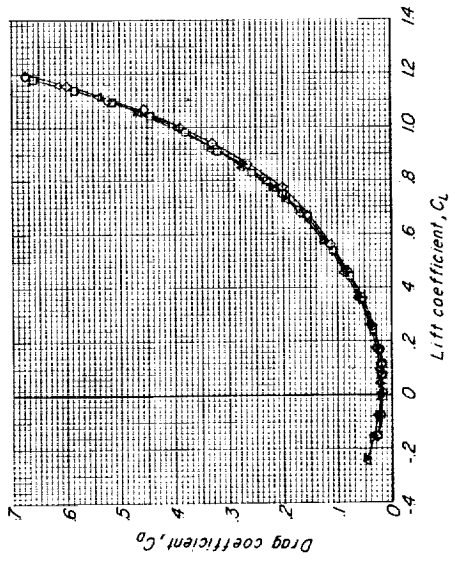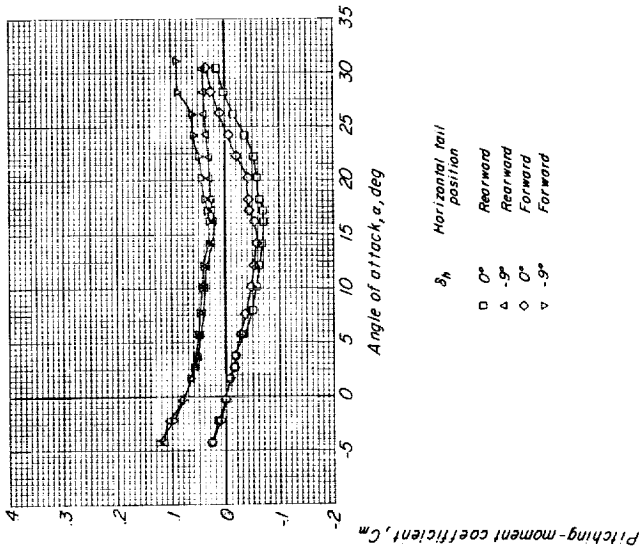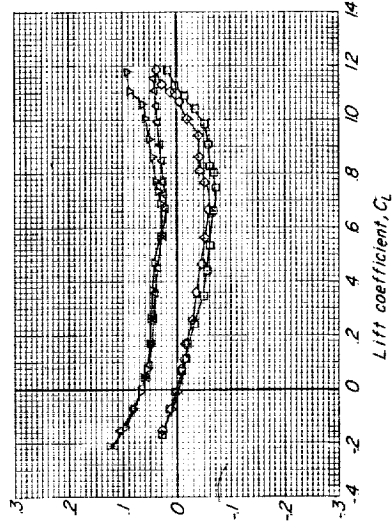
Figure 12.- Effect of horizontal-tail length on longitudinal aerodynamic characteristics. $\Lambda = 70°$ (leading edge extended); $S_h/S_w = 0.278$.
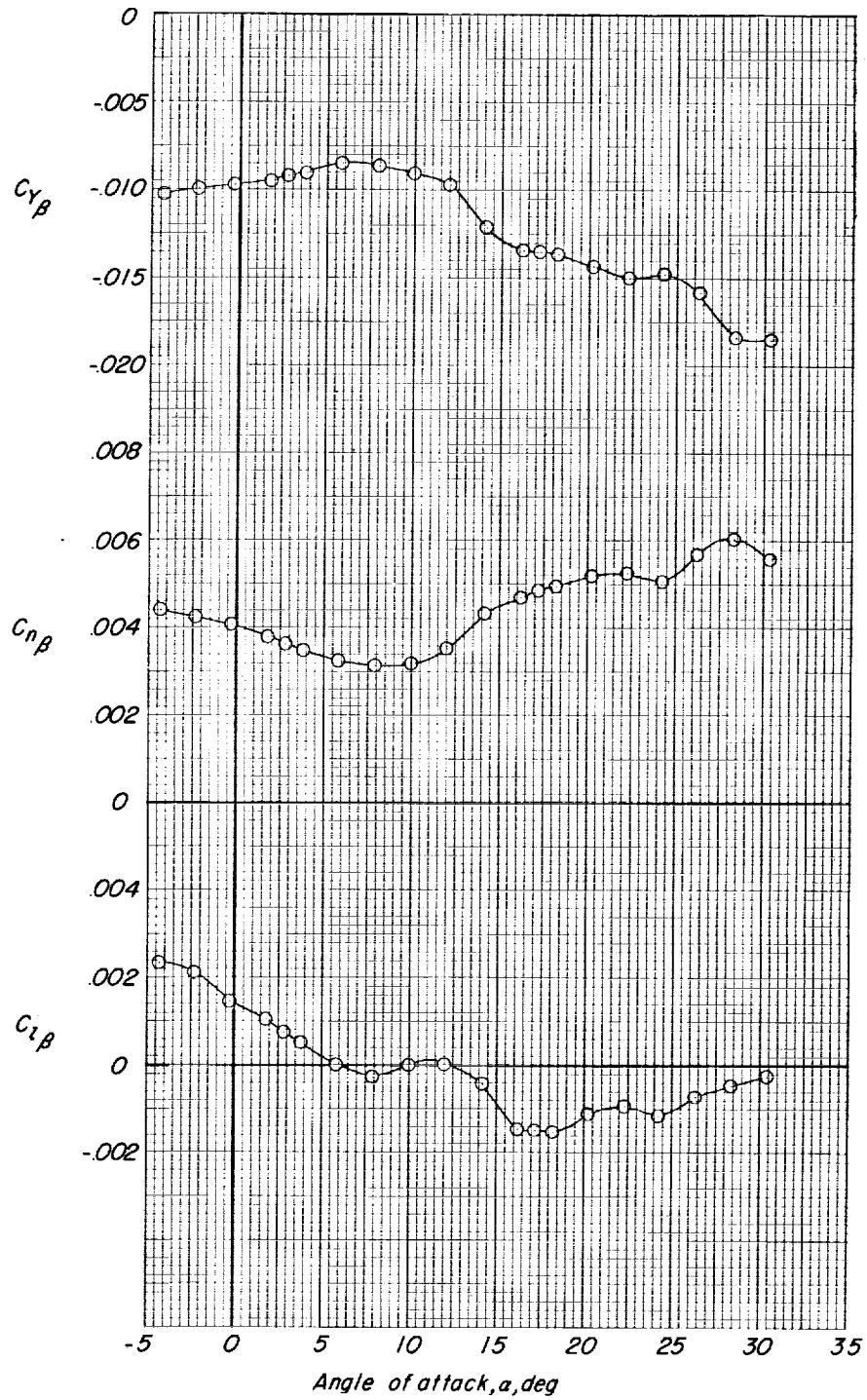
Figure 13.- The variation of the static lateral stability derivatives with angle of attack. $\Lambda = 70^\circ$; $S_h/S_w = 0.278$; $\delta_h = -9^\circ$.